Simulation of the Hysteresis Model for the MR Fluid Damper Using a Hybrid Evolutionary Algorithm

Xue Xiaomin

Department of Civil Engineering, Xi'an Jiaotong University, Xi'an, China

Wu Xiaohong

School of Aerospace, Xi'an Jiaotong University, Xi'an, China

Sun Qing

Department of Civil Engineering, Xi'an Jiaotong University, Xi'an, China

Zhang Ling

School of Aerospace, Xi'an Jiaotong University, Xi'an, China

The developed MF dampers can be used for diverse applications, including structural vibration mitigation, shock absorption, and vibration control in various systems. This paper has firstly investigated the mechanical characteristics of the self-made MR damper through experimentation. Based on the test data, the damper is found to possess nonlinear hysteresis. Usually, various models, especially the Bouc-Wen model, are proposed to interpret the complex characteristics which have the capability to capture behavior of a wide class of hysteretic systems. However, the Bouc-Wen model consists of a set of multi-unknown parameters that need to be estimated simultaneously. It is a burdensome task to effectively identify the exact values of the parameters. In view of this, this paper proposes a novel hybrid evolutionary algorithm combining Genetic Algorithm with Particle Swarm Optimization (GA-PSO). By using the GA-PSO, the optimized result would be more effective and accurate than the traditional one, because it overcomes the drawbacks of low-speed convergence in GA and local optimization in PSO. Finally it is verified through a large amount of experimental data, which can estimate the multi parameters in the Bouc-Wen model efficiently and precisely. Also suggested are the implications of the present study on other nonlinear hysteretic models or other complex mathematical models.

1. INTRODUCTION

Hysteresis is a memory-dependent, non-linear behavior in which the system output is not only dependent on the instantaneous input, but also on the past history of the input.[1,2] This type of inelastic behavior is encountered in many engineering fields, such as biology, electronics, ferroelectricity, mechanics, magnetism, etc. For efficient description of such inelastic systems, over the past years many mathematical models have been proposed for use in practical applications involving characterization of systems, identification or control.[3] The Bouc-Wen model[4] is widely used to describe systems with hysteresis and non-linear behavior, especially in civil and mechanical engineering. In this model, restoring force is related to the system viscous deformation through a first-order differential equation, which has a series of undefined parameters. By assigning proper values to these parameters, the response of the model will be in keeping with the actual behavior of hysteretic systems. Thus, it is pivotal to select an appropriate optimization algorithm to perform the task of parameter identification.

Recently, optimization techniques have been most widely applied to estimate the parameters of the Bouc-Wen model that characterize hysteretic behavior, such as Gauss-Newton and modified Gauss-Newton,[5] Levenberg-Marquardt,[6,7] Genetic Algorithms,[4,8] Particle Swarm Optimization,[9,10] etc. Traditional techniques (Gauss-Newton and Levenberg-Marquardt, etc.) are adequate to identify favorable parameters in the case of simple problems, since a good initial value can be easily obtained based on previous information. With regard to complex problems, favorable parameters cannot be identified with ease by local search algorithms due to the difficulties of setting the initial value.[8] As a result, parameter identification techniques based on intelligent algorithms are arousing more interest in modeling and parameter identification. For example, Genetic Algorithm (GA) and Particle Swarm Optimization (PSO) have robust features and are suitable for solving multi-objective problems. However, these methods also have their limitations. GA generally requires a large number of function evaluations whose convergence speed is quite slow because the evolution of solutions depends on evolutionary operators.[11] According to this situation, Liu focuses on the problem of premature convergence in GA, and proposes an adaptive GA based on population diversity.[10] Chang proposes an improved real-coded GA for parameter estimation of nonlinear systems to directly implement the programming operations.[12] Aine states that parameters of evolutionary algorithms should be appropriately

controlled for implementing an effective search, and a concept of dominance among control parameter vectors should be developed to show how it can be effectively used to reduce the storage.[13] In contrast to GA, PSO was reported to show better results in terms of computational time and cost,[12] but the problem of premature convergence is serious due to the lack of diversity where multiple objective function is concerned.[14] It is also sensitive to control parameter choices, especially the inertia weight, acceleration coefficients and velocity clamping. Incorrect initialization of these parameters may easily lead to divergence of cyclic behavior.[15]

In order to perfect the performance of intelligent algorithms, there have been some new ideas focusing on the hybrid PSO algorithm by adding GAs.[11,14,16] Simulations for a series of benchmark test functions show that the proposed method possesses better ability to find the global optimum with a relative high efficiency.[17] In this paper, a hybrid evolutionary algorithm combining the GA with PSO is proposed, called GA-PSO. In the GA-PSO, the part GA is improved by using an elitism strategy, and the part PSO is executed by an adaptive inertia weighting factor. At the same time, the GA-PSO is designed with an adaptive termination criteria. After these improvements are made, the proposed algorithm will achieve more accurate solutions with higher computational efficiency than traditional ones. In order to testify that the method is superior, we applied it to one classic multi-variate and multi-extremum function (*Shubert function*) to search for the minimum solution. Through comparing the results of the novel method with the Standard GA, it is found that the proposed approach is capable of much more accuracy and efficiency. In addition, parameter estimation of the Bouc-Wen model with noisy data is also considered, and its results are used to verify that the proposed approach is prominently robust and reliable. Finally, a large amount of experimental data of real MR damper is utilized to further validate the GA-PSO with satisfactory parameter estimation results and highly efficient computational capability.

This paper proposes a new promising identification method for highly nonlinear hysteretic systems described by using the Bouc-Wen model through adapting a novel hybrid evolutionary algorithm (GA-PSO). The paper is organized as follows: Section 2 introduces the self-made MR fluid damper and investigates its hysteretic behavior through experiment. Next, the Bouc-Wen model of the MR fluid damper and its parameter identification is introduced in section 3. In order to implement parameter identification effectively, a novel hybrid evolutionary algorithm is designed and proposed in Section 4. Section 5 discusses the efficiency and accuracy of the proposed approach. Finally, concluding remarks are given in Section 6.

2. MR FLUID DAMPER

The MR fluid damper is an ideal candidate in semi-active control for civil engineering structures. As is revealed by the introduction, the MR fluid damper has complex and dynamic mechanical characteristics. In this section, an experimental prototype of the MR fluid damper is designed and performed to obtain the necessary data for further study on modeling the hysteretic behavior using an appropriate algorithm.
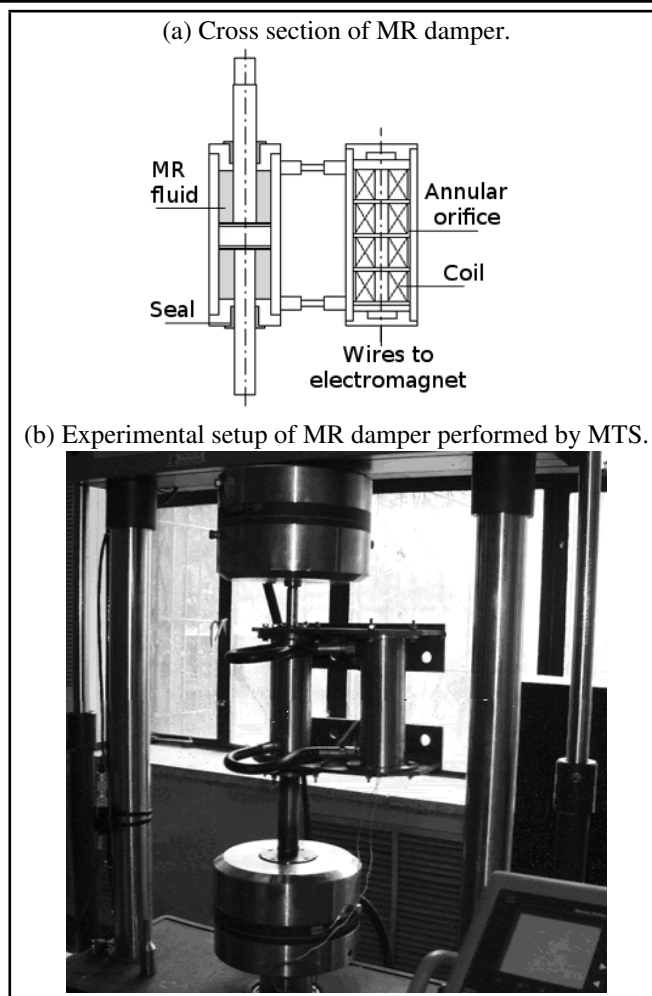

(a) Cross section of MR damper.

(b) Experimental setup of MR damper performed by MTS.

Figure 1. MR damper test setup.

2.1. Design of the MR Fluid Damper

As is shown in Fig. 1, a self-made MR fluid damper is performed by the Material Test System (MTS) at *State Key Laboratory for Strength and Vibration of Mechanical Structures in China*. We can see the schematic representation of the cylindrical type of MR damper in Fig. 1a. The MR fluid is housed within two cylinders: one is installed within the piston device, and the other is installed within electromagnets and coils. Within the piston device cylinder, the piston of the MR damper is driven by a two-way pusher-pull bar. When the magnetic field changes, the mechanical behavior of MR damper can be changed. As is exhibited in Fig. 1b, the actual damper is driven by a mechanical driver, and the generated force is measured by a force sensor.

2.2. Hysteresis Behavior of the MR Fluid Damper

By using the setup in Fig. 1, a series of preliminary tests are conducted to measure the response of the damper under various loading conditions. Fig. 2a displays partial cases of the damper's responses under 0.5 Hz and 2.0 Hz sinusoid excitation with the amplitude range fluctuating gradually from zero to ±10 mm, and the magnetic field varies as measured by the currents of 2.0 A.

It should be noted that the displacement-force curves are basically akin to ellipticals, suggesting that the relationship be-
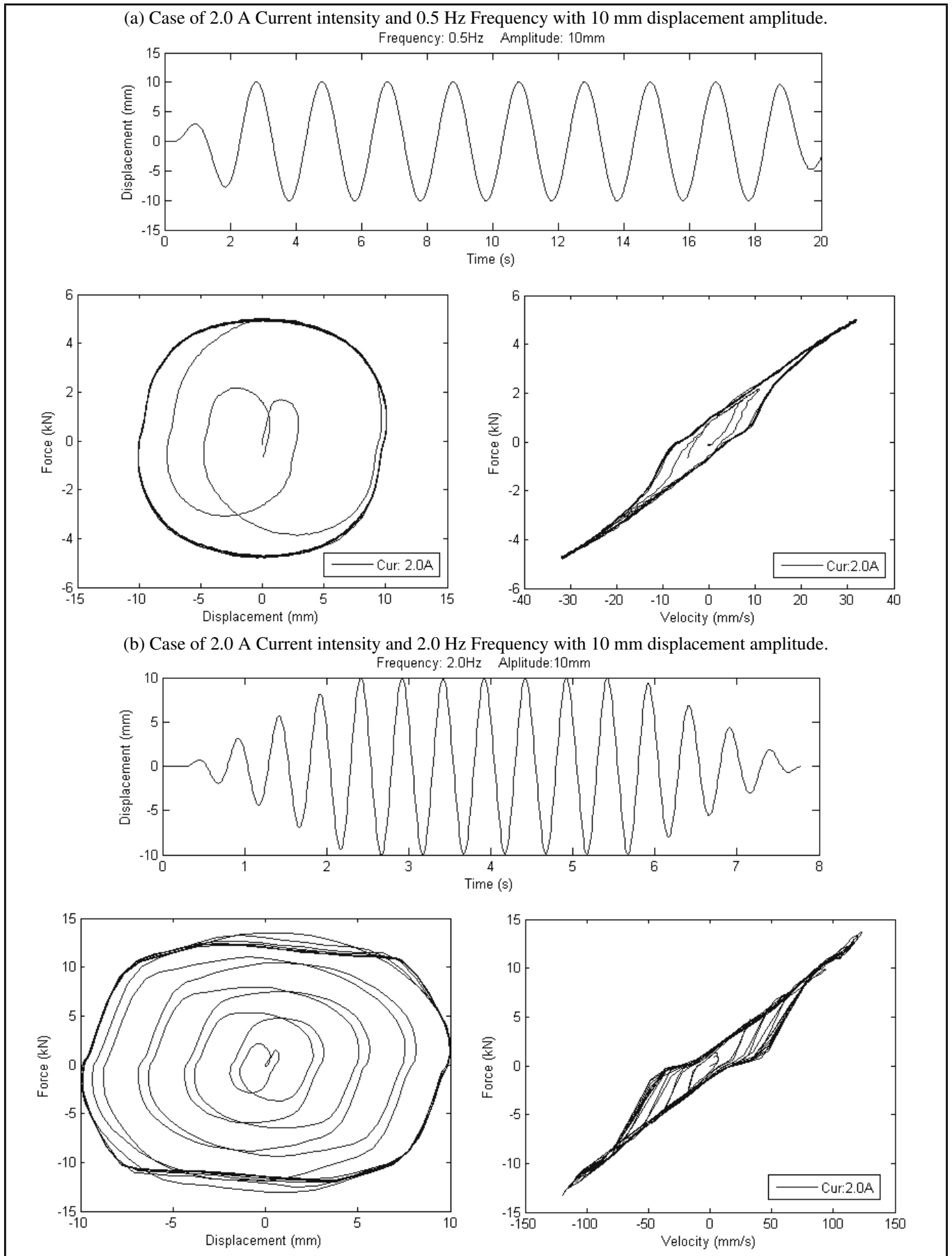
(a) Case of 2.0 A Current intensity and 0.5 Hz Frequency with 10 mm displacement amplitude.

(b) Case of 2.0 A Current intensity and 2.0 Hz Frequency with 10 mm displacement amplitude.

Figure 2. Hysteresis characteristic of the MR fluid damper.

tween displacement and force is nonlinear. Meanwhile as illustrated by the velocity-force curves in Fig. 2, their relationship is linear in high-velocity regions, but not in low-velocity regions centered at zero, appearing to be obvious hysteresis. As a result, the force-velocity relationship is characterized with obviously nonlinear hysteresis that should be much more paid attention. The above complex nonlinear hysteresis should be described accurately by an advanced model.

3. MECHANICAL MODEL OF THE MR FLUID DAMPER

The Bouc-Wen model is one of the important models used extensively for modeling various kinds of hysteretic systems. It has an important merit of being extremely versatile and can exhibit a wide variety of hysteretic behavior. In this paper, we mainly discuss how to make the Bouc-Wen model applicable to simulate the dynamic characteristic of the MR fluid damper.

3.1. Bouc-Wen Model

The normalized version of the Bouc-Wen model introduced in [4] relating the output $F(t)$ to the input $x(t)$ is given by

$$F(t) = c\dot{x}(t) + kx(t) + \alpha z(t) + f; \qquad (1)$$

where evolutionary variable z is governed by

$$\dot{z}(t) = Ax(t) - \beta\dot{x}(t)|z(t)|^n - \gamma|\dot{x}(t)|z(t)|z(t)|^{n-1}; \quad (2)$$

where c is the viscous coefficient contributing to the scaling relationship of the proportion by force and velocity, k is the stiffness contributing to the scaling relationship of the proportion by force and displacement, α is a scaling factor, and f is the initial damper displacement. As seen from the expressions, the characteristic parameters $c, k, \alpha, f, A, \beta, \gamma$ and n are undetermined in advance that should be identified by an optimization algorithm.

3.2. Parameter Analysis

Considering the nonlinear system governed by Eqs. (1) and (2), most of the parameters do not have clear physical meanings for damper's dynamic property.[8] When we employ one parallel algorithm to search for the optimal values of these parameters, initial settings such as searching ranges. for every parameter have an important effect upon the convergence rate and training speed of the algorithm. Moreover, these settings are generally designed based on their physical meanings to a large degree. For this reason, it is very imperative to discuss the contribution of every parameter to the Bouc-Wen model's output.

In order to explore the undetermined parameters playing what part of physical meaning or contribution for the hysteretic curves, different hysteretic curves are plotted in Fig. 3. The results are derived from numerical simulation of the Bouc-Wen model by a 4th order Runge-Kutta method with a time step $\Delta t = 0.01$ s. Herein, assume input x is harmonic displacement $x = Bsin(\omega t)$ where $\omega = \pi$ rad/s[1] and $B = 10$. The variables $x, \dot{x}, z$ and F and parameters $c, k, \alpha, f, A, \beta, \gamma$ and n in the Bouc-Wen model are temporarily supposed to be dimensionless. Various hysteretic curves are drawn in Fig. 3 by changing the values of every parameter. Based on their varying pattern, the parameters are analyzed below:

Table 1. Parameter description in Bouc-Wen model.

Parameters	Description
c	viscous factor
k	stiffness factor
α	Hysteretic factor
f	offset
A, β, γ	Shape control factor
n	Yield slope factor

- *Parameter c*: Fig. 3a shows that the original values of parameters $k, f, \alpha, A, \beta, \gamma$ and n are assumed to be fixed at 0.1, 0, 20, 0.1, 2, 2 and 1 respectively. Then, observe the curves' transformation along with the change of the parameter c. When the value of c is increased, we found that the displacement-force ($x - F$) curves become more distinctly full maintaining a certain slope. On the contrary, the average slope of the velocity-force ($\dot{x} - F$) curve, depicted by Fig. 3a, becomes larger when c does. Parameter c is susceptible to the relationship of velocity and force, and therefore it can be named "viscous coefficient".

- *Parameter k*: $c, f, \alpha, A, \beta, \gamma$ and n are assumed to be fixed at 0.1, 0, 20, 0.1, 2, 2 and 1 respectively. The value of k is susceptible to the relationship of displacement and generated force, and the average slope of the curve depicted by Fig. 3b becomes larger when k does. For this reason, k is always to represent the average slope of $x - F$ loops, which can be regarded as stiffness factor.

- *Parameter f*: The variety of the curves in Fig. 3c seems obviously simple. The force f is an offset that accounts for the nonzero mean value observed in the measured force.

- *Parameter α*: Its value is dependent on the hysteresis variable z which is a solution of the hysteresis differential z. Thus, it is very difficult to obtain an explicit value of α. The variety of the curves in Fig. 3d shows that α represents the ratio of linear to nonlinear responses, which is responsible for hysteretic characteristics.

- *Parameters A, β and γ*: The deformation of the curves seems analogous when A, β and γ vary severally (see Fig. 3e). They do not have a very clear physical meaning in general, which is the main reason that they match a wide class of hysteretic curves. Hence, we can call them shape control factors.

- *Parameter n*: As shown in Fig. 3f, it represents the sharpness of yield which controls the fullness of the hysteresis loops. In general, its value range is usually from 1 to 3.

Based on the above analysis, it is concluded that the common definition of these parameters in the Bouc-Wen model is suitable for the MR fluid damper in Table 1.

3.3. Parameter Identification

The Bouc-Wen model comprises two equations, one of which is a differential equation concerning the intermediate variable z. Since the expressions are obviously complex, for convenience, Bouc-Wen mathematic equations can be described by a discrete form, such as

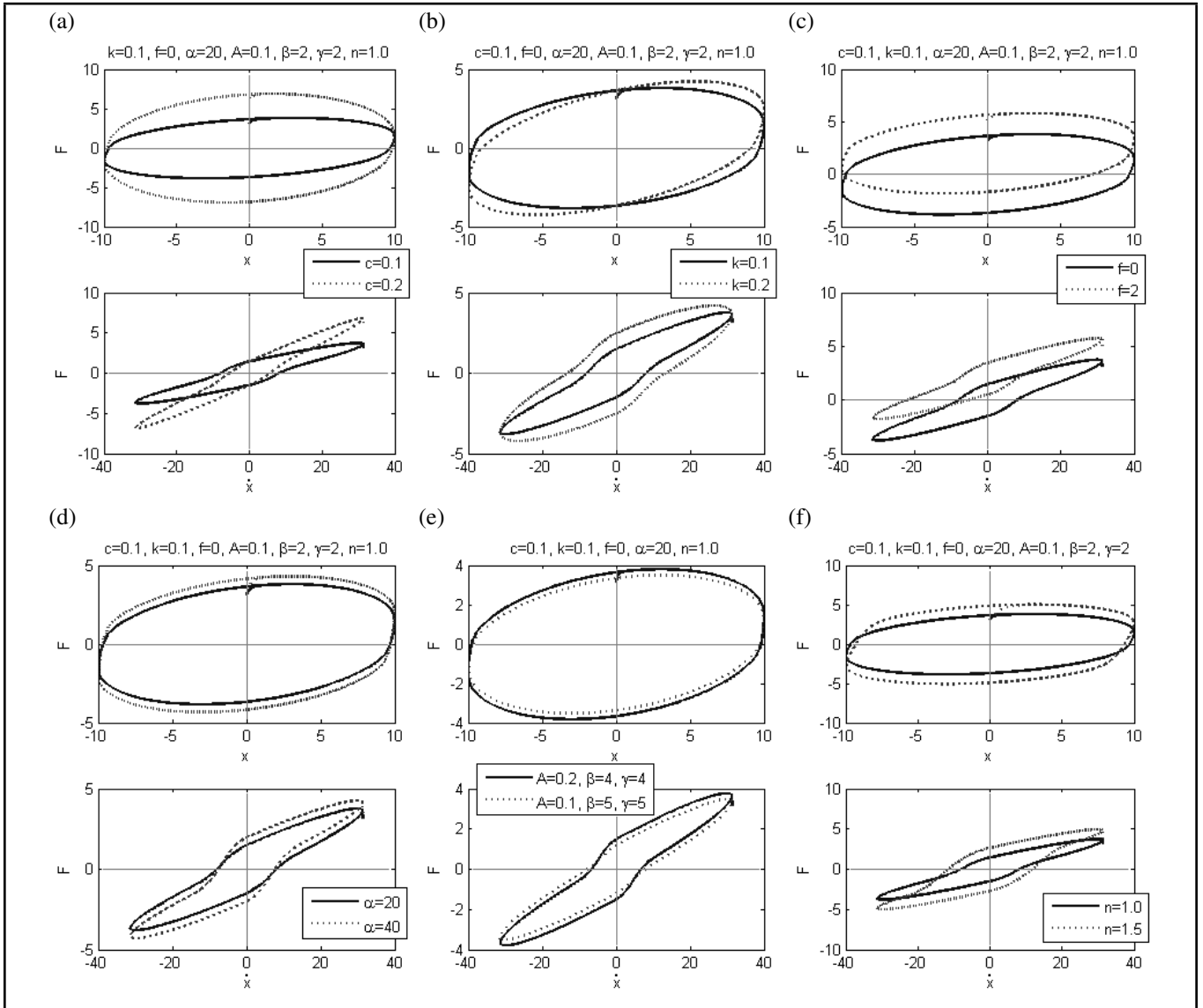$$F_{sim}(k) = f(x(k), \dot{x}(k), z(k), \Theta); \qquad (3)$$

Figure 3. Examples of hysteresis curves generated by the Bouc-Wen model with different parameters.

where F_{sim} is simulated force and $\Theta = [c, k, f, \alpha, A, \beta, \gamma, n]$ is a set of identified parameters of the Bouc-Wen model, and $x/\dot{x}$ is the damper displacement/velocity derived from experimental data.

We also assume the responses of one hysteretic system or device to be a Bouc-Wen model. Then the system can be expressed by

$$F_{\exp}(k) = f(x(k), \dot{x}(k), z(k), \Theta_0); \qquad (4)$$

where F_{exp} is damper force derived from experimental data, and Θ_0 is a set of original parameters representing the inherent characteristics of the hysteretic systems, which must be found out by an advanced parallel algorithm.

A flow chart on the parallel algorithm for parameter estimation of the Bouc-Wen model is depicted in Fig. 4. Its process is introduced as follows: At first, experimental data, including damper displacement x and velocity $\bar{x}$, were collected and incorporated into the Bouc-Wen model formulation expressed in Eqs. (1) and (2). Accordingly, the simulated MR damper force F_{sim} was figured out. During this phase of the parallel algorithm, the objective function was defined as the sum of differences between the MR damper force of experimental results
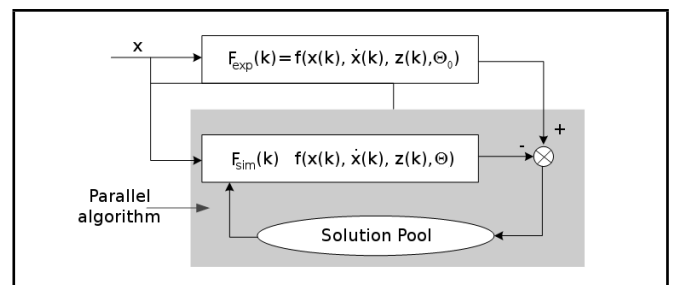

Figure 4. The procedure of parameter estimation by Parallel Algorithm.

and those of the simulated results. It can thus be concluded that, the lower the objective function value, the better the estimated parameters. Through appropriate iterative circulation, the best results will eventually be picked out.

4. HYBRID EVOLUTIONARY ALGORITHM

4.1. Modified GA

As a powerful computational search and optimization tool, the GAs have been applied successfully to problems in many fields such as optimization design, fuzzy logic control, neural

networks, expert systems, scheduling and many others.[4, 8, 18] Generally, GA procedure consists of three basic factors: chromosome structure, fitness function, and some control parameters (select operator, crossover operator, etc.). The standard GA implementation was generally in its standard form, using a fixed number of generations for iteration and with predetermined crossover and mutation rates. However, the algorithm efficiency was not adequately considered in the GA. With the development of GA, variations to the traditional procedures were proposed in a large amount of literature. By setting appropriate control-parameters, they will conspire to make optimization results more accurate and effective. In this paper, a computationally-efficient GA is proposed firstly.

4.1.1. Chromosome Structure

Chromosome structure mainly depends on the nature of the problem to be solved. In the case of the solution structure of parameter estimation of the Bouc-Wen model, there are altogether eight undetermined parameters ($c, k, f, \alpha, A, \beta, \gamma$ and n) in Eqs. (1) and (2). Therefore, the chromosome can be

$$\Theta_i = \{c_i, k_i, f_i, \alpha_i, A_i, \beta_i, \gamma_i, n_i\}, i = 1, ..., N; \quad (5)$$

where N is the maximum of chromosomes and i is the ith individual in chromosome.

4.1.2. Elitism Strategy

The lowest fitness obtained in the chromosome during the GA iteration is stored so as to ensure the offspring of the best chromosome in subsequent generations.[19] Generally, standard GA uses the roulette wheel strategy to reserve the relative "good" individuals for next circle based upon the values of individual fitness function. However, this method easily arouses some vital problems such as "low efficiency" and "local optimization," because of its random search property.[20] Drawing on this, we can reserve the fittest individual in each generation without undergoing crossover and mutation progress, which can converge to the global optimum. When the generation evolves, the minimum error (elite individual) will directly approach the global optimum. That is

$$e_{min}^{i+1} \le e_{min}^i; \quad (6)$$

where e_{min}^i is the minimum error (elite individual) at the i th generation. "e" can be designed by the distance between the simulation and experiment results of damper forces. In this paper, we choose the fitness function as the error "e" (see Eq. (10)). As a result of the elitism strategy, the value of the error function is descending to zero directly. The stored minimum errors cannot increase over iterations.

Unlike the standard GA implementation where the best individual (chromosome) might be lost due to encountered stochastic effects, the iterative process in improved GA is always searching for the universal best solution at the minimum error rate since the strategy can remove the destructive effect of the crossover and mutation. Consequently, the tendency of descending errors is successfully maintained and the efficiency of the algorithm is greatly enhanced.

4.2. Modified PSO

Swarm intelligence is an exciting new research field still in its infancy compared to other paradigms in artificial intelligence. A number of computational swarm-based systems have been developed in the past decade, where the approach is to model the very simple local interactions among individuals, from which complex problem-solving behaviors emerge.[21]

Suppose that the searching space is D-dimensional and n particles form the colony. The i th particle represents a D-dimensional vector $X_i(i = 1, 2, \ldots, n)$ that stands for the i th particle location $X_i = (x_{i1}, x_{i2}, ..., x_{iD})(i = 1, 2, ..., n)$ in the searching space. In the PSOs, the location vector $x^{(t+1)_{id}}$ at the next time step is given by

$$x_{id}^{(t+1)} = x_{id}^{(t)} + v_{id}^{(t+1)}; \quad (7)$$

where $x_{id}^{(t)}$, $v_{id}^{(t+1)}$ are the location at the current time step and the velocity at the next time step for the i th particle and d th dimensional vector.

We should calculate the particle's fitness value by putting its location into a designated objective function that is analogous to the process of GA. When the value of the fitness is higher, the corresponding X_i is more "excellent". The velocity vectors are adjusted to move toward the previous best position of each particle and that of a swarm, defined as

$$v_{id}^{(t+1)} = \omega v_{id}^{(t)} + c_1 r_1 (P_{id} - x_{id}^{(t)}) + c_2 r_2 (P_{gd} - x_{gd}^{(t)}); \quad (8)$$

where $i = 1, 2, \ldots, n$, $d = 1, 2, \ldots, D$, r_1 and r_2 are uniformly distributed random numbers ($r_1, r_2 \in [0, 1]$), and c_1 and c_2 are learning rates controlling the effects of the personal and global guides, respectively, while ω is the inertia weight controlling the balance between exploration and exploitation, and it is the following decreasing linear function:

$$\omega(t) = \omega_{\max} - (\omega_{\max} - \omega_{\min})\frac{t}{t_{\max}}; \quad (9)$$

where ω_{max} and ω_{min} are the final weight and initial weight respectively. The equation is meant to decrease the diversification characteristic of particles within a certain velocity, which guarantees the searching point gradually approximate to P_{id} and P_{gd}. In this paper we set the values of ω_{max} and ω_{min} equal to 0.9 at the beginning of the search and 0.4 at the end of the search respectively, according to the empirical study.[5] By using a linearly-decreasing inertia weight, the PSO will be ameliorated greatly in contrast to the cases where the inertia weight is a positive constant. Like the improved GA, the fitness function fit is equal to the objective function RMSE as in Eq. (10).

4.3. Hybrid Evolutionary Algorithm

GA and PSO are basically similar in their inherent parallel characteristics, whereas experiments display that they have their respective advantages and disadvantages. This paper is set out to present a hybrid evolutionary algorithm, by combining the advantages of GA and PSO. This algorithm can highlight the excellent features of GA and PSO while avoiding the weaknesses, such as low calculation efficiency in GAs and premature convergence in PSOs.

In hybrid evolutionary algorithm, the appropriate objective function and termination rule should be designed as are introduced as below.

4.3.1. Fitness Function

A fitness function is a measuring mechanism that is used to evaluate the status of every individual or particle. Each goes through the same evaluating exercise. The key to directly influencing the final identified results is in designing an appropriate identified function. This paper employs the Root-Mean-Square Error (RMSE), herein to be taken as the fitness function, which is governed by

$$fit = \frac{1}{n}\sqrt{\sum_{i=1}^{n}\left(F_{sim,i} - F_{\exp,i}\right)^2}; \qquad (10)$$

where n is the number of data points, and each simulation/experimental data point is indexed by subscript $sim,i/exp,i$.

4.3.2. Termination Rule

An early evolutionary algorithm generally terminates after the expiry of a fixed number of terminations. However, when the solution has already found the minimum error but not yet arrived at the designated generation, it is undoubtedly time-consuming to go on iterating. For this reason, an appropriate termination rule should be created so as to relieve the unnecessary computational burden.

The termination strategy in this study is proposed under two aspects: one is depending on maturity degree of the population proceeding in a certain generation. Another is in view of the fittest individuals after iterating a certain generation, controlling the real calculation accuracy.

Rule 1: Terminate the GA-PSO if a reduction of minimum error lower than 20% of maximum error does not arise in further generation, which is defined as

$$e_{\min}^k - e_{\min}^{k+1} \leqslant 0.2 \max_k\{e_{\min}^k\}; \qquad (11)$$

where e_{min}^k represents the minimum error in k th generation. This rule can guarantee that the population should not be diversified any more, and the best individual is very close to the global solution.

Rule 2: Terminate the GA-PSO if the minimum fitness value is below a threshold e_{min}, which is given by

$$fit_{\min} \leqslant e_{\min}; \qquad (12)$$

where e_{min} is the designated threshold value of fitness, and fit_{min} represents the minimum fitness value in individuals. This rule can guarantee the final solution's precision is adequately satisfied.

The flowchart of the hybrid evolutionary algorithm is introduced in Fig. 5. Firstly, the initial population is randomly generated according to structural optimization problems, and then the objective function is utilized to evaluate the status of each individual or particle in the population. Based on the evaluation results, the population is divided into two sub-populations. Within the population, 50% of the individuals with lower fitness are input to the GA-based identifier to identify the unknown parameters. Simultaneously, another 50% with higher fitness are input to the PSO. The above allocation scheme can ensure improving the convergence speed of GA, while avoiding plunging into local optimum in PSO. The process will be
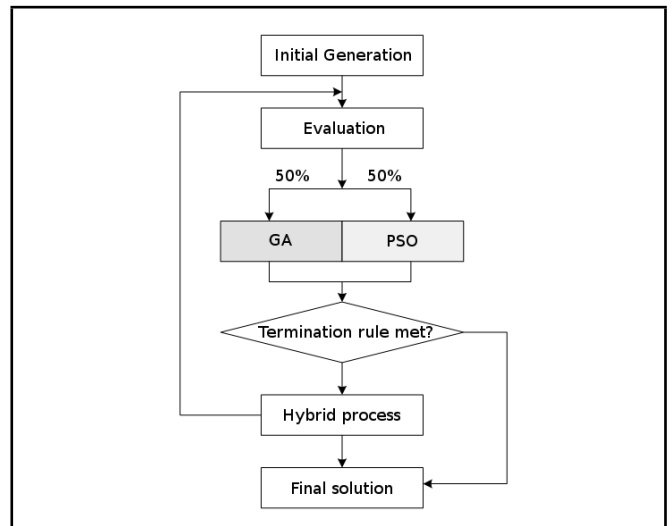

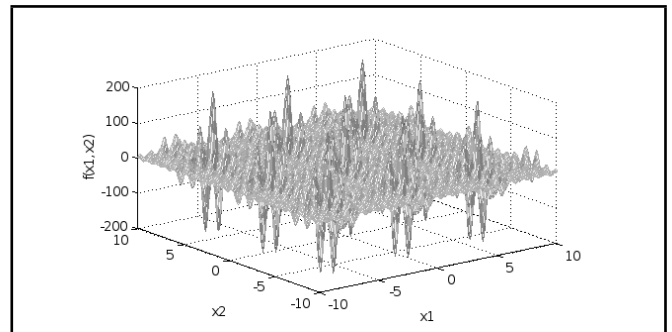**Figure 5.** Flow chart of hybrid evolutionary algorithm.

Figure 6. *Shubert* functions graph.

repeated until one solution can satisfy the requirement of the termination rule, and it should be exacted to be the final or optimal solution.

4.4. Validation in Test Function Problems

The performance of the hybrid evolutionary algorithm was evaluated by multi-variable, multi-model function problem that is known as the *Shubert* function. The test function is as follows:

Optimize the minimum in $f(x_1, x_2) =$

$$\sum_{i=1}^{5} i\cos[(i+1)\cdot x_1 + i] \cdot \sum_{i=1}^{5} i\cos[(i+1)\cdot x_2 + i];$$
$$x_1, x_2 \in [-10, 10].$$

The *Shubert* function graph in Fig. 6 displays multiple peaks. If Standard GA or PSO is used, the best solution will usually search for the local minimum value of the function. Avoiding the problems of "premature" and "local optimization" is an arduous task that should be settled successfully. In order to prove the superiority of the proposed approach, we applied the Standard GA and the GA-PSO respectively to solve the minimum value of the *Shubert* function, and their efficiencies and accuracies are compared to each other.

Note that the standard GA is performed using the following algorithm settings: roulette wheel selection, crossover rate $P_c = 0.85$, mutation rate $P_m = 0.01$, and the maximum gener-

Table 2. Test data of *Shubert* function minimization.

min $f(x_1, x_2)$	Generation					
	5	10	25	30	40	50
Standard GA	-110.3478	-162.8241	-186.2324	-186.6189	-185.8875	-186.7301
GA-PSO	-183.4561	-186.7098	-186.7306	–	–	–

ation $N = 50$. Both in the standard GA and GA-PSO, the number of population/particles is a set of 80. The above-mentioned approach has been implemented by MATLAB. Simulation is processed by an Intel Core2 Duo E6300 1.86 processor with 1024M RAM, under Windows 7.

Figure 7 illustrates that the value of the fitness function experiences an approximate descending course as optimization processes both in the Standard GA and GA-PSO. It is observed in Fig. 7a that the first twelve generations finish more than 90% of the convergence in the iterative process, and the further reduction in estimation error is in the region of gentle slope. There is no more evolution after the 16th generation when the error is reaching the minimum value. Thus, it is very crucial to establish an appropriate termination rule which can get rid of redundant iterative generations in due time. When GA-PSO adopts the termination *Rule 1* and *Rule 2*, the process shows a very quickly descending tendency, only experiencing twenty-five generations, and the best solution (-186.7306) is found out. Meanwhile, by comparison between the average solution experiences with standard GA and GA-PSO, the solution range in GA-PSO is a little farther from the final solution than result in the standard GA. This is because the average solution is mainly dependent on the dispersion degree of the individuals in optimization algorithms. If the individuals were more diversified, the average solution would be more decentralized. In this sense, the generated individuals in GA-PSO are much more diversified, resulting in one global optimized solution. Thus, a more accurate solution in GA-PSO will be obtained, which is also verified in Table 2.

As illustrated in Table 2, the minimum value of the *Shubert* function by using Standard GA is -186.7301 in the 50th generation. With regard to the GA-PSO, the minimum value maintains -186.7306 in the 25th generation. Obviously, a smaller number of generations are required, and higher accuracy is obtained by the GA-PSO before termination. In view of this, we recommend the hybrid evolutionary algorithm (GA-PSO) for solving complex problems because of its high precision and efficiency.

5. IDENTIFICATION RESULT AND DISCUSSION

In order to implement numerical calculation for the Bouc-Wen model, a 4th order Runge-Kutta method is adopted to solve the differential Eq. (2) with a time step $\Delta t = 0.02$ s. Assuming that the excitation function is harmonic displacement $x = 10 sin(\pi t)$ (where the unit is mm), some typical solutions of the mechanical formulation are shown in Fig. 8.

In this study, the first case that was considered original values of eight parameters ($c_0, k_0, f_0, \alpha_0, A_0, \beta_0, \gamma_0, n_0$) are assumed to be fixed at 0.08 kN·s/mm, 0.01 kN/mm, 0 kN, 20 kN/mm, 0.05, 4 kN·s/mm$^{2.8}$, 2 kN·s/mm$^{2.8}$ and 1.8 respectively. Likewise the second case is considered that original values of parameters are assumed to be fixed at 0.1 kN·s/mm, 0.01 kN/mm, 2.0 kN, 25 kN mm, 0.05, 4 kN·s/mm$^{2.5}$, 2 kN·s/mm$^{2.5}$ and 1.5 respectively.
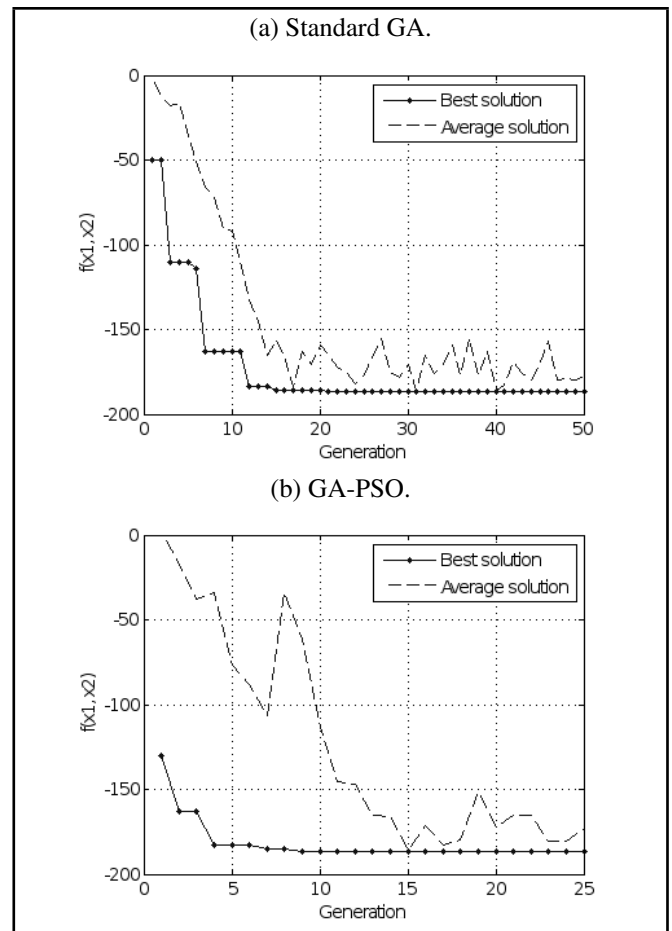

Figure 7. Iterative track of the best and average fitness values.

5.1. Noise-free Estimation

Firstly, we consider noise-free estimation, in which force data is not corrupted. In order to validate the superiority of the GA-PSO, it is compared with the Standard GA in terms of the accuracy and efficiency of the results. The Standard GA is performed using the following algorithm settings: roulette wheel selection, crossover rate $P_c = 0.85$, mutation rate $P_m = 0.01$, and the maximum generation $N = 30$.

Statistics of the estimated parameters with case 1 and case 2 are illustrated in Table 3 and Table 4, respectively. Furthermore, we also compare the accuracy and efficiency between the Standard GA and the GA-PSO in Table 5. The errors in the GA are 0.1351 kN on average, the process of which is terminated in the 30th generation. Regarding the GA-PSO, however, the average errors are less than 0.0933 kN , and its process is terminated within the 16th generation. Obviously, the GA-PSO requires a smaller number of generations but obtains results with much greater accuracy.

As shown in Fig. 9, it is found that the hysteretic loops are in very close agreement with the simulated hysteresis. Note that the original curves are plotted by solid lines, and the estimated results are plotted by a series of small circles. In Fig. 10, the errors between the original and estimated damper force values
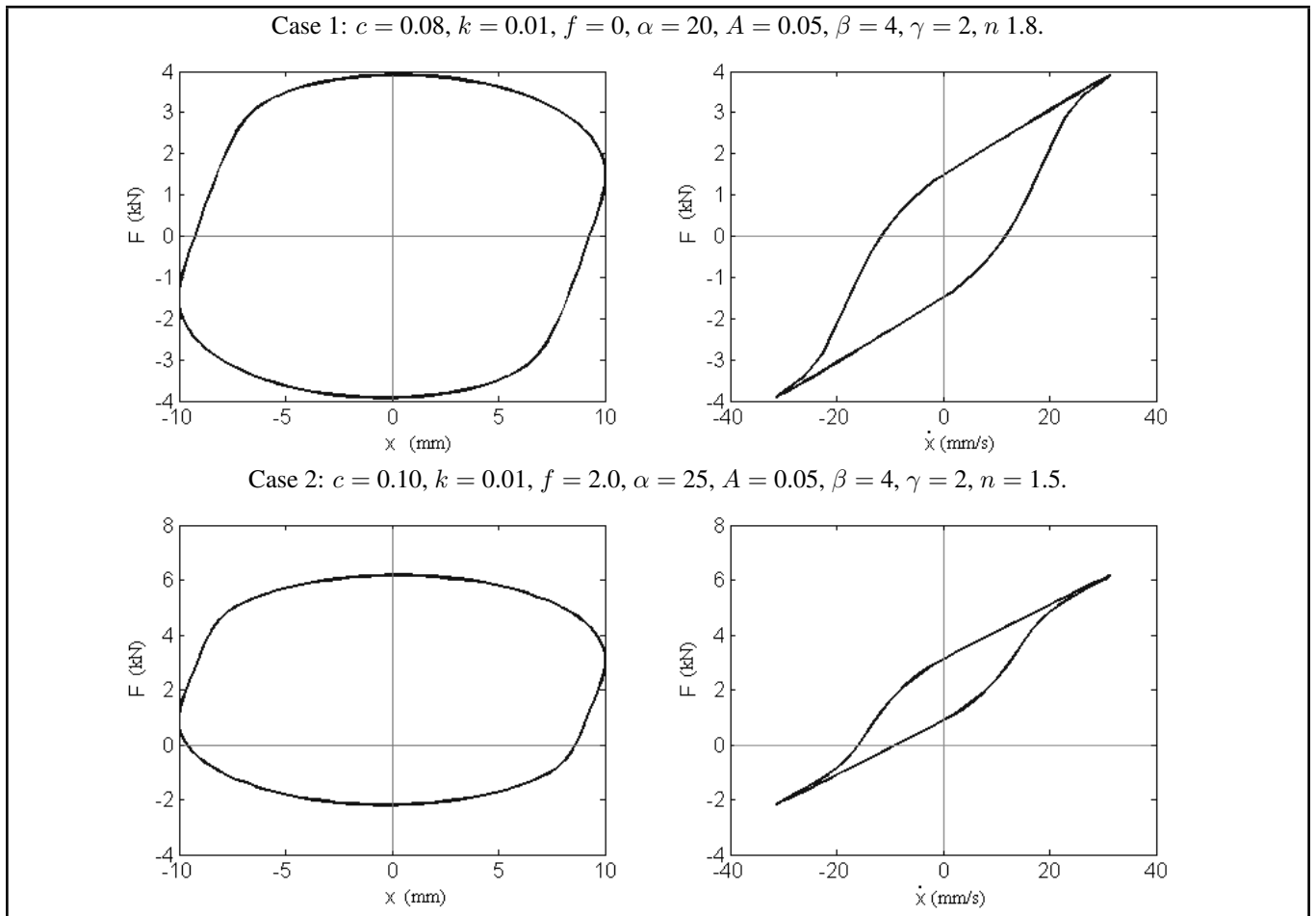
Figure 8. The hysteresis loops generated by the Bouc-Wen model.

Table 3. Comparisons of estimated parameters from the case 1 by using Standard GA and GA-PSO.

Estimated by	Original	Standard GA	GA-PSO
c (kN·s/mm)	0.08	0.0849	0.0817
k (kN/mm)	0.01	0.0157	0.0241
f (kN)	0	0.0568	0.0146
α (kN/mm)	20	15.9478	16.7831
A (dimensionless)	0.05	0.0573	0.0673
β (kN·s/mm^{n+1})	4	1.4041	3.1223
γ (kN·s/mm^{n+1})	2	2.2604	2.0178
n (dimensionless)	1.8	1.7031	1.7167
RMSE (kN)	N/A	0.1425	0.0933

Table 4. Comparisons of estimated parameters from the case 2 by using Standard GA and GA-PSO.

Estimated by	Original	Standard GA	GA-PSO
c (kN·s/mm)	0.1	0.1087	0.1018
k (kN/mm)	0.01	0.0148	0.0201
f (kN)	2	1.9717	2.0311
α (kN/mm)	25	19.9222	16.2741
A (dimensionless)	0.05	0.0416	0.0774
β (kN·s/mm^{n+1})	4	3.2460	2.7106
γ (kN·s/mm^{n+1})	2.00	2.3371	3.1919
n (dimensionless)	1.5	1.5981	1.5362
RMSE (kN)	N/A	0.1277	0.074

can also be surveyed, and maintain less than 0.2 kN everywhere.

5.2. Noise Estimation

Next, parameter estimation of the Bouc-Wen model with a set of noisy data is considered. In the real parameter estima-

Table 5. Comparison of accuracy and efficiency by using Standard GA and GA-PSO with original data.

	Standard GA		GA-PSO	
	RMSE (kN)	Generation	RMSE (kN)	Generation
Case 1	0.1425	30	0.0933	15
Case 2	0.1277	30	0.0740	16
Average	0.1351	30	0.0836	15.5

tion problem of the model, measured data are often corrupted by noise. Then uncertainty can arise from measurement instruments, system noise, low-accuracy calculation, etc. Thus, the effect of noise should be taken into account. In this paper, a series of random values are added to the original data. Assume x' is noise data, and then it can be divided two parts:

$$x' = x + x_n \xrightarrow{Bouc-Wen} F' = F + F_n; \qquad (13)$$

where x represents the component of original data, and x_n represents the component of additive noise at each particular time. Through substituting x' for x in Bouc-Wen model, a set of damper force data F' is obtained subsequently. Then the RMSE function Eq. (10) can be replaced by

$$fit = \frac{1}{n} \sqrt{\sum_{i=1}^{k} \left(F_{sim,i} - F'_i\right)^2}; \qquad (14)$$
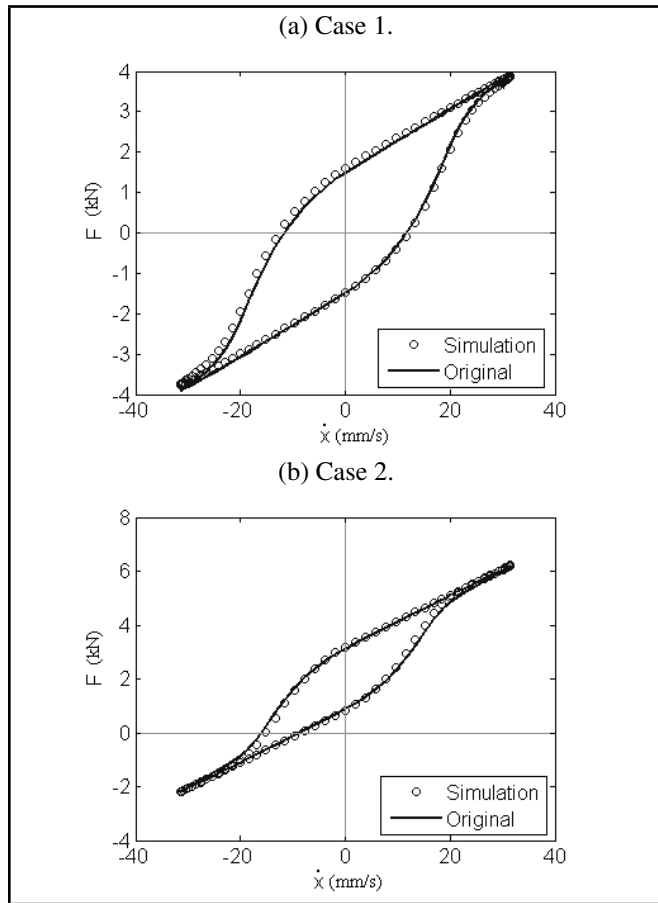
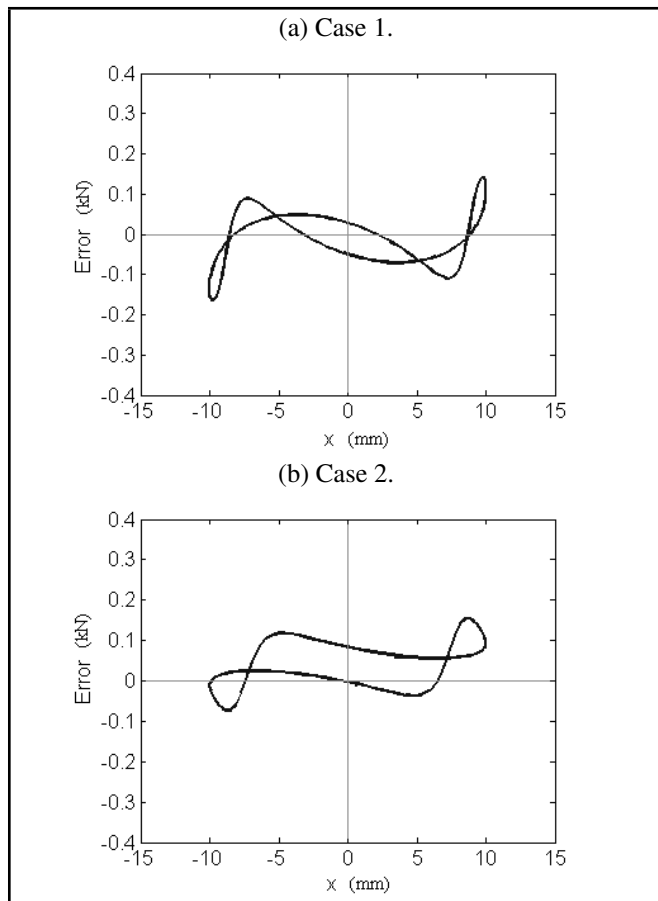**Figure 9.** Parameter estimation results using the GA-PSO.
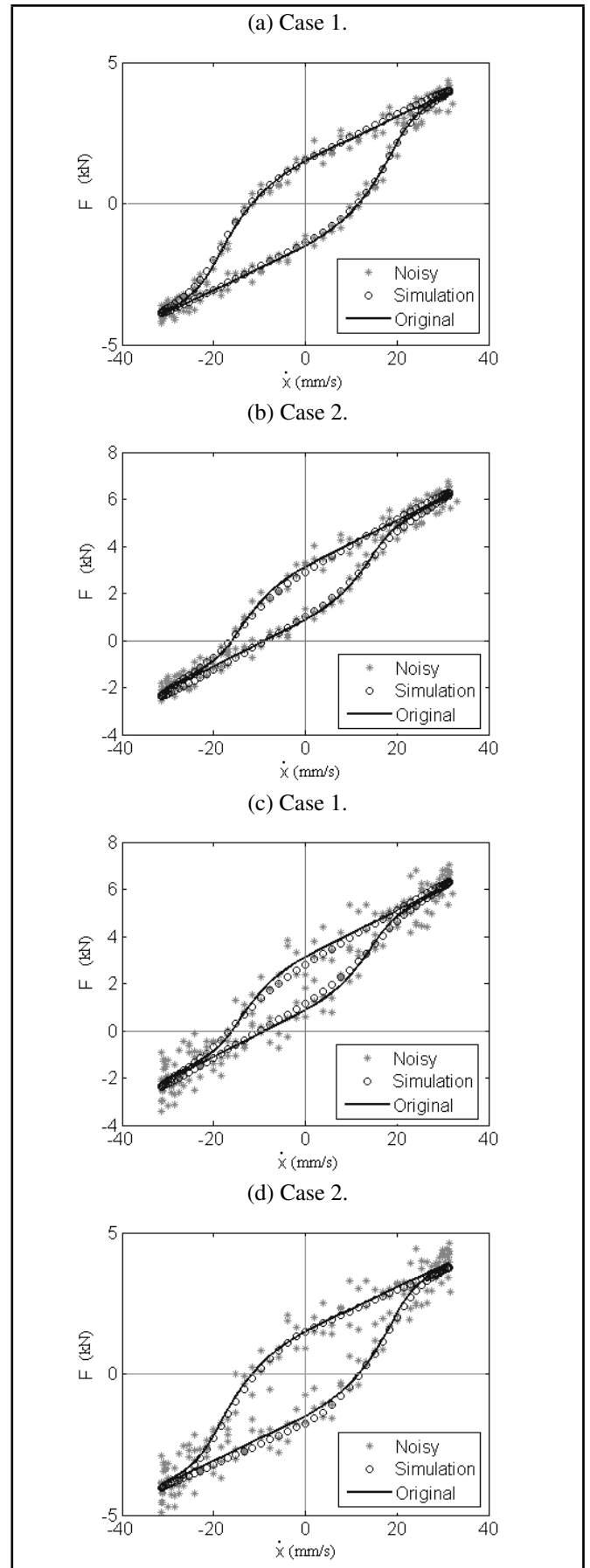

Figure 10. Errors by using GA-PSO.

Figure 11. Parameter estimation by the GA-PSO with noisy data at (a),(b)10% and (c),(d)25% levels of NR.

In this study, the percentage noise ratio is designed to perform optimization for different level noise. The noise ration (NR) is given by

$$NR = \frac{1}{n} \sum_{i=1}^{n} (\frac{x_i - x_i'}{\bar{x}}) \times 100\%; \qquad (15)$$

where n is the number of data points, each data point is indexed by subscript i, and $\bar{x}$ represents the average value of original data .

Some numerical results of hysteretic loops simulated using GA-PSO with noise data are displayed in Fig. 11, in which the estimation curves appear to remain quite close to the original one. This proves that the proposed method is effective, even if the original data are corrupted by different degrees of noise.

By collecting a large amount of examples shown in Table 6 and Table 7, most of the estimated parameter values differ from the original values, and there exist different errors under different degrees of noise. When the noise ratio becomes bigger, the error will increase. It should be noted that the errors are basically below 0.2 kN, even if the noise ratio reaches up to 40%.

5.3. Simulation of a Real MR Damper

In the experiment, the damper behavior of the MR damper is observed under 0.5 Hz, 1.0 Hz and 2.0 Hz sinusoid excitation with 10 mm amplitude displacement, and the magnetic field is varied by different currents ranging from 0 A to 3.0 A. In Figure 2, the damping curves from experimental data are not very smooth, which should be interfered by a certain degree of noises, possibly arising from measurement instruments, system noise, etc. The noise existing in hysteretic curves will impose more difficulties on construction for an effective Bouc-Wen model with accurate identified parameters. In this paper, a large amount of experimental data obtained from the MR fluid damper is utilized to verify that the proposed approach has the capability to estimate the satisfactory parameters of the Bouc-Wen model efficiently. We also compare it with Standard GA in terms of accuracy and efficiency. (Herein the Standard GA is performed using the following algorithm settings: roulette wheel selection, crossover rate $P_c = 0.85$, mutation rate $P_m = 0.01$, and the maximum generation $N = 60$.)

In the proposed method, several sets of identified parameters are figured out due to different applied current intensities, which are shown in Table 8. By using Standard GA, the average errors are 0.1254 kN, 0.1766 kN and 0.2701 kN under the frequency of 0.5 Hz, 1.0 Hz and 2.0 Hz, respectively. Regarding the GA-PSO, however, the average errors are less than 0.1012 kN, 0.1214 kN and 0.2 kN, and their processes are terminated in the 35th, 40th, and 42th generation, respectively. In GA-PSO, the solution is quite precise, where its errors are consistently below 0.2 kN . In addition, the GA-PSO represents higher computational efficiency whose iteration are around forty generations.

In the proposed method, the typical results are drawn in different cases of 0.5 Hz, 1.0 Hz and 2.0 Hz frequency with different current intensities from 0 A to 3 A. Each case has the sinusoidal displacement of 10 mm. Part of the calculation values of the estimated parameters are listed in Table 9. As exhibited in Fig. 12, it merits great attention that the nonlinear hysteresis responses are in large agreement with theexperimental data by

Table 6. Estimated parameters from case 1 with noisy data.

NR (%)	10	20	30	40
c (kN·s/mm)	0.0791	0.0837	0.0958	0.0760
k (kN/mm)	0.0228	0.0300	0.0315	0.0015
f (kN)	0.0159	0.0224	0.0379	0.0626
α (kN/mm)	17.4237	27.5348	15.5224	28.6553
A (dimensionless)	0.0492	0.0273	0.0387	0.0412
β (kN·s/mm^{n+1})	1.0009	2.6252	4.3346	3.6241
γ (kN·s/mm^{n+1})	4.2481	2.6995	3.9699	3.8054
n (dimensionless)	1.8955	1.7282	1.9878	1.8416
RMSE (kN)	0.1237	0.1345	0.1520	0.1982

Table 7. Estimated parameters from case 2 with noisy data.

NR (%)	10	20	30	40
c (kN·s/mm)	0.0979	0.1101	0.1121	0.1105
k (kN/mm)	0.0092	0.0147	0.0180	0.0083
f (kN)	1.9020	1.9618	1.8989	2.0804
α (kN/mm)	22.0790	23.0376	15.5506	21.7743
A (dimensionless)	0.0592	0.0251	0.0375	0.0234
β (kN·s/mm^{n+1})	4.7363	2.5276	1.6250	4.9113
γ (kN·s/mm^{n+1})	2.9286	4.9258	3.1510	3.8106
n (dimensionless)	1.6124	1.6960	1.5912	1.7903
RMSE (kN)	0.1015	0.1304	0.1640	0.1892

using GA-PSO method. It is intended to testify that the results of the proposed method are very satisfactory.

6. CONCLUSION

This paper reports on an experimental study of the MR damper, the results of which indicate that the MR damper has the remarkably nonlinear hysteretic characteristic. Usually the Bouc-Wen model is utilized to model the hysteretic characteristic. However, the Bouc-Wen model consists of a set of multi-unknown parameters that need to be estimated simultaneously. It is a burdensome task to effectively identify the exact values of the parameters. In view of this, this paper proposes a novel hybrid evolutionary algorithm combining Genetic Algorithm with Particle Swarm Optimization (GA-PSO). The simulation results verify the GA-PSO has the ability to search for the global optimal solution with remarkable computational accuracy and efficiency. Finally, a series of preliminary data obtained from a real MR damper is used to again testify that the proposed method is capable of estimating the satisfactory parameters of the Bouc-Wen model efficiently. It makes sense to predict that the approaches presented herein can also throw light on the development and characterization of other complex hysteretic systems.

ACKNOWLEDGMENT

REFERENCES

[1] Talatahari, S., Kaveh, A. and Rahbari, N. M. Parameter identification of Bouc-Wen model for MR fluid dampers using adaptive charged system search optimization, *Journal of Mechanical Science and Technology*, **26**, 2523–2534, (2012).

[2] Su, C. Y., et al. Adaptive variable structure control of a class of nonlinear systems with unknown Prandtl-Ishlinskii
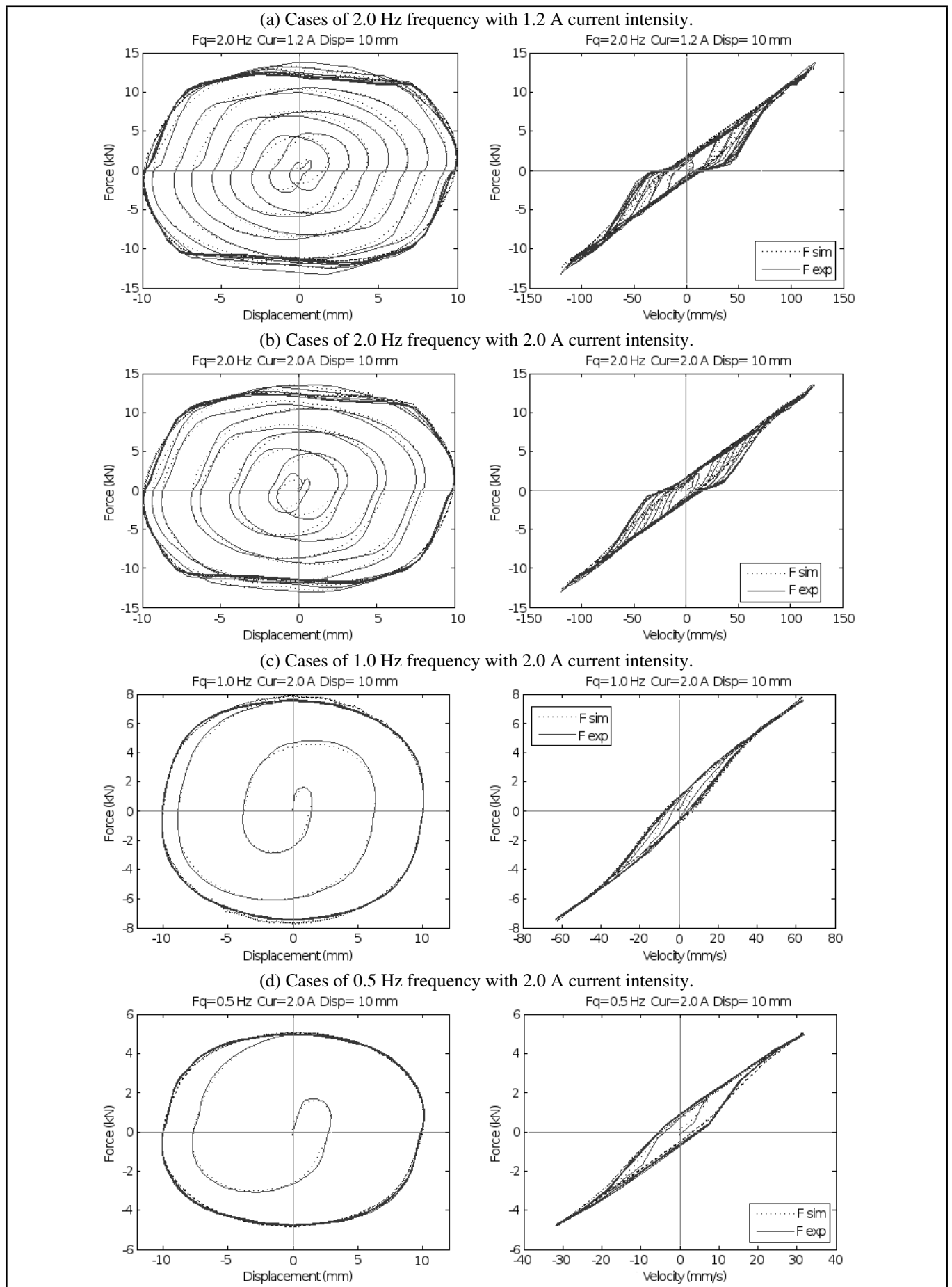
Figure 12. Comparison of experimental data and simulation result using GA-PSO.

Table 8. Comparison of accuracy and efficiency by using Standard GA and GA-PSO with experimental data.

Current	Standard GA			GA-PSO		
	RMSE (kN)/Generation			RMSE (kN)/Generation		
(A)	0.5 Hz	1.0 Hz	2.0 Hz	0.5 Hz	1.0 Hz	2.0 Hz
0.0	0.1088/60	0.1322/60	0.2182/60	0.0906/36	0.1070/39	0.1988/42
1.0	0.1345/60	0.1656/60	0.2355/60	0.1034/35	0.1252/40	0.2018/43
2.0	0.1230/60	0.1544/60	0.2858/60	0.1011/38	0.1378/41	0.1975/43
3.0	0.1220/60	0.1935/60	0.2656/60	0.0995/32	0.1416/42	0.2235/46
Average	0.1254/60	0.1766/60	0.2701/60	0.1012/35	0.1214/40	0.2000/42

Table 9. Results of estimated parameters from experimental data by GA-PSO.

Estimated parameters	0.5Hz				1.0Hz			
	0 A	1.0 A	2.0 A	3.0 A	0 A	1.0 A	2.0 A	3.0 A
c (kN·s/mm)	0.0814	0.1280	0.1379	0.1361	0.0829	0.0965	0.1077	0.1137
k (kN/mm)	0.0069	0.0053	0.0186	0.0156	0.0046	0.0097	0.0131	0.0074
f (kN)	0.0719	0.0867	0.1191	0.1099	0.1089	0.0953	0.0843	0.0855
α (kN/mm)	21.9454	22.2498	24.1578	23.5827	21.1473	22.0022	22.3648	22.6112
A (dimensionless)	0.0514	0.0437	0.0443	0.0614	0.0294	0.0512	0.0653	0.0436
β (kN·s/mm^{n+1})	1.9969	3.3321	1.9265	2.8253	4.3092	3.8721	2.1201	1.1962
γ (kN·s/mm^{n+1})	3.2880	2.1538	2.2603	1.1420	1.9211	3.5864	4.6584	4.8255
n (dimensionless)	1.3057	1.4044	1.2311	1.1510	1.3002	1.4021	1.4152	1.4440

hysteresis, *IEEE Transactions on Automatic Control*, **50**, 2069–2074, (2005).

[3] Ismail, M., Ikhouane, F. and Rodellar, J. The hysteresis Bouc-Wen model, a survey, *Archives of Computational Methods in Engineering*, **16**, 161–188, (2009).

[4] Kwok, N. M., et al. Bouc-Wen model parameter identification for a MR fluid damper using computationally efficient GA, *ISA Transactions*, **46**, 167–179, (2007).

[5] Kunnath, S. K., Mander, J. B. and Fang, L. Parameter identification for degrading and pinched hysteretic structural concrete systems, *Engineering Structures*, **19**, 224–232, (1997).

[6] Zhang, H., et al. Parameter identification of inelastic structures under dynamic loads, *Earthquake Engineering & Structural Dynamics*, **31**, 1113–1130, (2002).

[7] Ni, Y. Q., Ko, J. M. and Wong, C. W. Identification of non-linear hysteretic isolators from periodic vibration tests, *Journal of Sound and Vibration*, **217**, 737–756, (1998).

[8] Xue, X. M., et al. Semi-active control strategy using genetic algorithm for seismically excited structure combined with MR damper, *Journal of Intelligent Material Systems and Structures*, **22**, 291–302, (2011).

[9] Ye, M. and Wang, X. Parameter estimation of the Bouc–Wen hysteresis model using particle swarm optimization, *Smart Materials and Structures*, **16**, 2341, (2007).

[10] Charalampakis, A. E. and Dimou, C. K. Identification of Bouc–Wen hysteretic systems using particle swarm optimization, *Computers & Structures*, **88**, 1197–1205, (2010).

[11] Sivanandam, S. N. and Deepa, S. N. Introduction to genetic algorithms, Springer, (2007).

[12] Habib, S. J. and Al-kazemi, B. S. Comparative study between the internal behavior of GA and PSO through problem-specific distance functions, *The 2005 IEEE Congress on Evolutionary Computation*, **3**, 2190–2191, (2005).

[13] Dimian, M. and Andrei, P. Noise induced resonance phenomena in stochastically driven hysteretic systems, *Journal of Applied Physics*, **109**, 07D330–07D330, (2011).

[14] Jeong, S., et al. Development and investigation of efficient GA/PSO-hybrid algorithm applicable to real-world design optimization, *Computational Intelligence Magazine, IEEE*, **4**, 36–44, (2009).

[15] Li, Y. and Xu, Q. Adaptive sliding mode control with perturbation estimation and PID sliding surface for motion tracking of a piezo-driven micromanipulator, *IEEE Transactions on Control Systems Technology*, **18**, 798–810, (2010).

[16] Assareh, E., et al. Application of PSO (particle swarm optimization) and GA (genetic algorithm) techniques on demand estimation of oil in Iran, *Energy*, **35**, 5223–5229, (2010).

[17] Shi, X. H., et al. An improved GA and a novel PSO-GA-based hybrid algorithm, *Information Processing Letters*, **93**, 255–261, (2005).

[18] Juang, C. F. A hybrid of genetic algorithm and particle swarm optimization for recurrent network design, *IEEE Transactions on Systems, Man, and Cybernetics, Part B: Cybernetics*, **34**, 997–1006, (2004).

[19] Rudolph, G. Convergence analysis of canonical genetic algorithms, *IEEE Transactions on Neural Networks*, **5**, 96–101, (1994).

[20] Knjazew, D. OmeGA: A competent genetic algorithm for solving permutation and scheduling problems, Springer, (2002).

[21] Kennedy, J. Particle swarm optimization, *In Encyclopedia of Machine Learning*, Springer US, (2010).